

## EXTRACTING PLANET MASS AND ECCENTRICITY FROM TTV DATA

YORAM LITHWICK<sup>1</sup>, JIWEI XIE<sup>2</sup>, & YANQIN WU<sup>2</sup>

*Draft version November 27, 2024*

### ABSTRACT

Most planet pairs in the Kepler data that have measured transit time variations (TTV) are near first-order mean-motion resonances. We derive analytical formulae for their TTV signals. We separate planet eccentricity into free and forced parts, where the forced part is purely due to the planets' proximity to resonance. This separation yields simple analytical formulae. The phase of the TTV depends sensitively on the presence of free eccentricity: if the free eccentricity vanishes, the TTV will be in phase with the longitude of conjunctions. This effect is easily detectable in current TTV data. The amplitude of the TTV depends on planet mass and free eccentricity, and it determines planet mass uniquely only when the free eccentricity is sufficiently small. We proceed to analyze the TTV signals of six short period Kepler pairs. We find that three of these pairs (Kepler-18,24,25) have TTV phase consistent with zero. The other three (Kepler-23,28,32) have small TTV phases, but ones that are distinctly non-zero. We deduce that the free eccentricities of the planets are small,  $\lesssim 0.01$ , but not always vanishing. Furthermore, as a consequence of this, we deduce that the true masses of the planets are fairly accurately determined by the TTV amplitudes, within a factor  $\lesssim 2$ . The smallness of the free eccentricities suggests that the planets have experienced substantial dissipation. This is consistent with the hypothesis that the observed pile-up of Kepler pairs near mean-motion resonances is caused by resonant repulsion. But the fact that some of the planets have non-vanishing free eccentricity suggests that after resonant repulsion occurred there was a subsequent phase in the planets' evolution when their eccentricities were modestly excited, perhaps by interplanetary interactions.

### 1. INTRODUCTION

The Kepler mission has detected an abundance of low-mass close-in planets (Batalha et al. 2012). Remarkably, hundreds of them are members of planetary systems (Lissauer et al. 2011; Fabrycky et al. 2012b). These will likely prove to be a Rosetta stone for deciphering the dynamical history of planetary systems.

One of the most intriguing Kepler discoveries is that, while the spacing between planets in a system appears to be roughly random, there is a distinct pile up of planet pairs just wide of certain resonances, and a nearly empty gap just narrow of them (Lissauer et al. 2011; Fabrycky et al. 2012b). In Lithwick & Wu (2012), we proposed that dissipation is responsible for this asymmetry, via an effect we termed “resonant repulsion” (also see the independent work by Batygin & Morbidelli 2012). The eccentricity of planets near resonances can be separated into two parts: a part that is forced by the resonance and is determined by the planets' proximity to resonance (*forced eccentricity*), and a part that is unrelated to the resonance (*free eccentricity*)<sup>3</sup>. If there is dissipation, it damps away the planets' free eccentricities, but the forced eccentricities persist as long as the planets remain close to resonance. As the dissipation continually acts on these forced eccentricities, it extracts energy from the planets' orbits, and

in doing so pushes apart any planet pair that happens to lie near a resonance (Lithwick & Wu 2008; Papaloizou 2011). Hence all such planet pairs end up just wide of resonance, naturally explaining the Kepler result.

If it is indeed resonant repulsion that is responsible for the pile up – and to date no other tenable mechanisms have been proposed – then there are a number of interesting implications. First, it implies that before resonant repulsion occurred the distribution of spacings was nearly uniform, i.e., that planet pairs were placed with little regard for resonances. Second, it implies that most of the Kepler planets suffered a prolonged bout of eccentricity damping. Third, it implies that the free eccentricities of the planets should be zero today, after the prolonged bout of dissipation. This prediction can be tested using the transit time variations (TTV) recorded by Kepler, as we demonstrate in this paper.

A transiting planet that has no companion transits at perfectly periodic times. But one that has a companion deviates slightly from its periodic schedule because of the gravitational tugs from its companion. Agol et al. (2005) and Holman & Murray (2005) proposed using TTV signals to characterize the companions of transiting extrasolar planets, and this technique has proved to be highly successful both for confirming Kepler candidates and for measuring their masses and eccentricities (e.g., Cochran et al. 2011; Ford et al. 2012; Steffen et al. 2012; Fabrycky et al. 2012a). However, all these studies rely on fitting the observed TTV signals to direct N-body simulations (e.g. Veras et al. 2011). Such fits are computationally costly. Moreover, N-body simulations do not provide a dynamically transparent interpretation of the system.

Here, we focus on near-resonant pairs because the nearly coherent interactions in such pairs induce particularly large TTV signals. Such pairs account for most

<sup>1</sup> Dept. of Physics and Astronomy, Northwestern University, 2145 Sheridan Rd., Evanston, IL 60208 & Center for Interdisciplinary Exploration and Research in Astrophysics (CIERA)

<sup>2</sup> Department of Astronomy and Astrophysics, University of Toronto, Toronto, ON M5S 3H4, Canada

<sup>3</sup> Our forced eccentricity is perhaps more accurately called the forced resonant eccentricity to distinguish it from the more commonly used forced *secular* eccentricity (e.g., Murray & Dermott 2000). But only the resonant contribution plays a role in this paper.

of the TTV detections to date in the Kepler database. Motivated by our earlier work on resonant repulsion, we separate the eccentricity into free and forced parts. Interestingly, in so doing, the expression for the TTV near first-order resonance becomes particularly simple.

This paper is organized as follows. In Section 2, we present new analytical formulae for the TTV from two near-resonant planets, and show that the results agree with N-body simulations. In Section 3, we apply the TTV formulae to six planet pairs with published TTV data. In Section 4, we discuss our findings and their implications.

## 2. PLANET PARAMETERS FROM ANALYTICAL TTV

We consider the TTV signals from two coplanar planets that lie near (but not in) a  $j:j-1$  mean motion resonance. The results are derived in the Appendix, and summarized in the following. Let  $\delta t \equiv O - C$  be the inner planet's transit time delay, where  $O$  is the observed transit time and  $C$  is calculated from the linear ephemeris under the assumption that transits are perfectly periodic. Similarly,  $\delta t'$  is the outer planet's time delay. We show in the Appendix that

$$\delta t = \frac{V}{2i} e^{i\lambda^j} + c.c. = |V| \sin(\lambda^j + \angle V) \quad (1)$$

$$\delta t' = \frac{V'}{2i} e^{i\lambda'^j} + c.c. = |V'| \sin(\lambda'^j + \angle V'), \quad (2)$$

where  $V = |V|e^{i\angle V}$  and  $V' = |V'|e^{i\angle V'}$  are the complex TTV (expression in Eqs. 8-9), and are nearly constant; c.c. denotes the complex conjugate of the preceding term; and

$$\lambda^j \equiv j\lambda' - (j-1)\lambda, \quad (3)$$

is the *longitude of conjunctions* (e.g., Agol et al. 2005), where  $\lambda$  and  $\lambda'$  are the mean longitudes of the inner and outer planet, respectively. At the order of approximation to which we work (see Appendix), we may set

$$\lambda = \frac{2\pi}{P}(t - T), \quad \lambda' = \frac{2\pi}{P'}(t - T') \quad (4)$$

in Equation (3), where  $P$  and  $P'$  are the periods of the inner and outer planet, and  $T$  and  $T'$  are offsets; all four of these parameters are constant. The actual mean longitudes differ slightly from the above expressions if the planets are eccentric (and that is included in the TTV derivation).

Equations (1)–(2) show that TTV signals are sinusoidal, with a period determined by  $\lambda^j$ . We call this the *super-period*:

$$P^j \equiv \frac{1}{|j/P' - (j-1)/P|}. \quad (5)$$

There is a simple geometrical interpretation to  $\lambda^j$ . Since  $\lambda$  and  $\lambda'$  are approximately the angular positions of the inner and outer planets,  $\lambda^j$  gives the angular position of both planets whenever they hit conjunction ( $\lambda = \lambda'$ ). Furthermore,  $\lambda^j$  progresses linearly in time between conjunctions. For a near-resonant pair, successive conjunctions differ only slightly in angular position, and hence their super-period is very long. More precisely, we define

the normalized distance to resonance

$$\Delta \equiv \frac{P'}{P} \frac{j-1}{j} - 1, \quad (6)$$

in which case the super-period is

$$P^j = \frac{P'}{j|\Delta|}. \quad (7)$$

For example, a planet pair that has a period ratio of 2.02 is at a distance of  $\Delta = 0.01$  from the 2:1 resonance, and its super-period is 50 times longer than the outer planet's orbital period. A pair of planets that have  $\Delta > 0$  lie wide of resonance, and their  $\lambda^j$  decreases with time (i.e., is retrograde with respect to the orbital motion); conversely, a pair with  $\Delta < 0$  lie narrow of resonance and their  $\lambda^j$  is prograde.

Henceforth it will prove convenient to measure angles with respect to the line of sight. In that case,  $\angle V$  and  $\angle V'$  are the phases of the TTV signals relative to the time when the longitude of conjunction points along the line of sight ( $\lambda^j = 0$ ). In addition, the offsets  $T$  and  $T'$  then have the interpretation of being the time of any particular transit of the inner and outer planet, respectively.

In the Appendix, we derive the expressions for the complex TTV:

$$V = P \frac{\mu'}{\pi j^{2/3} (j-1)^{1/3} \Delta} \left( -f - \frac{3}{2} \frac{Z_{\text{free}}^*}{\Delta} \right), \quad (8)$$

$$V' = P' \frac{\mu}{\pi j \Delta} \left( -g + \frac{3}{2} \frac{Z_{\text{free}}^*}{\Delta} \right), \quad (9)$$

where  $\mu$  is the mass ratio of the inner planet to the star and  $\mu'$  that of the outer planet, and  $f$  and  $g$  are sums of Laplace coefficients with order-unity values, as listed in Table 3. Note that  $f < 0$  and  $g > 0$ . When the pair is far from resonance,  $|\Delta|$  is order unity, and the TTV expression reduces to  $\sim P\mu$ . The key new dynamical quantity that controls the TTV signal is

$$Z_{\text{free}} \equiv f z_{\text{free}}' + g z_{\text{free}}', \quad (10)$$

(with  $Z_{\text{free}}^*$  its complex conjugate), which is a linear combination of the free complex eccentricities of the two planets. We proceed to define and describe the important concept of free eccentricity.

### 2.1. Free Eccentricity

The complex eccentricity of a planet is

$$z = e e^{i\varpi}, \quad (11)$$

where  $\varpi$  is the longitude of periaapse. Near a first-order mean-motion resonance, this can be decomposed into free and forced parts,

$$z = z_{\text{free}} + z_{\text{forced}}. \quad (12)$$

The planet's forced eccentricity is forced by virtue of its companion's proximity to resonance. For the inner and outer planets,

$$\begin{pmatrix} z_{\text{forced}} \\ z_{\text{forced}}' \end{pmatrix} = -\frac{1}{j\Delta} \begin{pmatrix} \mu' f (P/P')^{1/3} \\ \mu g \end{pmatrix} e^{i\lambda^j}, \quad (13)$$

(Eq. A15). In the case  $\Delta > 0$ , the forced eccentricity of the inner planet is aligned with the longitude of conjunc-

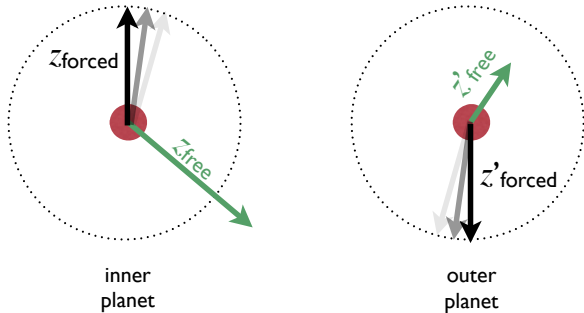


FIG. 1.— Schematic of free and forced complex eccentricities of a pair of near-resonant planets. The complex eccentricity for each planet is a sum of free and forced components. The free component is constant (on timescales  $\ll$  secular times) with arbitrary amplitude and phase. The forced component has magnitude determined by the planets’ proximity to resonance, and phase that rotates in parallel with the longitude of conjunctions  $\lambda^j$ , with a super-period  $P^j = P'/|j\Delta|$ .

tions, and that of the outer planet is anti-aligned. The situation is reversed for  $\Delta < 0$ .

The free eccentricities can take arbitrary values. They represent the degrees of freedom associated with the non-circularity of the orbits. Although there are four such degrees of freedom (corresponding to  $e, \varpi, e', \varpi'$ ), they can only affect the TTV signal through the linear combination of Equation (10). The complex free eccentricities precess on the secular timescale,  $\sim P/\mu$ , which is much longer than the super-period. So during any short timespan TTV observation, they can be taken as constant. See Fig. 1 for a cartoon illustration of these concepts.

## 2.2. Interpreting TTV

Given two transiting planets, how much can be learnt about their parameters from measuring their TTV? The analytical expressions allow for straightforward answers, sparing one the abstruseness of N-body simulations. If both transits are observed, then  $P, P', T, T'$  are known, even in the absence of observed TTV. These yield  $\Delta$  and  $\lambda^j$ . The TTV signals then allow one to measure four quantities, the real and imaginary parts of  $V$  and  $V'$  (via Eqs. 1–2). Therefore the four unknown parameters ( $\mu, \mu'$ , and the real and imaginary parts of  $Z_{\text{free}}$ ) could in principle be inferred by inverting Equations (8)–(9). However, as we discuss in the following, degeneracies often arise that prevent unique inversion.

The *amplitudes* of the complex TTV are

$$|V| \sim P \frac{\mu'}{|\Delta|} \left(1 + \frac{|Z_{\text{free}}|}{|\Delta|}\right). \quad (14)$$

$$|V'| \sim P' \frac{\mu}{|\Delta|} \left(1 + \frac{|Z_{\text{free}}|}{|\Delta|}\right), \quad (15)$$

after dropping order-unity coefficients; we also assume for the purposes of the present discussion that  $|Z_{\text{free}}/\Delta|$  is either very large or very small ( $\gg 1$  or  $\ll 1$ ). We infer that the TTV amplitude of the inner planet yields an upper limit on the mass of the outer planet,  $\mu' \lesssim |\Delta||V|/P$ , and there is a corresponding limit on the inner planet’s mass.<sup>4</sup> But the value of  $\mu'$  cannot be extracted from the TTV amplitude without knowing the value of  $|Z_{\text{free}}|$ :

<sup>4</sup> The TTV amplitude yields the mass if  $|Z_{\text{free}}/\Delta| \ll 1$  and an upper limit on the mass if  $|Z_{\text{free}}/\Delta| \gg 1$ . But if  $|Z_{\text{free}}/\Delta| \sim \text{unity}$ , then the mass could greatly exceed that nominal upper limit pro-

a smaller  $\mu'$  can be compensated for by a higher  $|Z_{\text{free}}|$  without affecting the amplitude of  $V$ . Similarly, if both planets have measured TTV’s, one can determine the ratio of their masses from the TTV amplitudes (within order unity constants), but not the mass of either individually, without knowing  $|Z_{\text{free}}|$ .

Can the *phases*<sup>5</sup> be used to determine mass and free eccentricity uniquely? This is in general impossible. From Equations (8)–(9), the two planets’ TTV signals are exactly out of phase with each other (anti-correlated) in either the limit that  $|Z_{\text{free}}| \ll |\Delta|$  or  $|Z_{\text{free}}| \gg |\Delta|$ . This feature has been noted before and has been used to help confirm some Kepler planets (Steffen et al. 2012). In either limit, TTV signals only provide three independent quantities ( $|V|, |V'|$  and one phase), and hence a degeneracy remains between planet mass and free eccentricity. To break it, additional information or assumptions are required, e.g., radial velocity measurements or the stability of the planetary system (Cochran et al. 2011; Fabrycky et al. 2012a). An alternative solution would be if TTV phases can be measured very accurately to discern the small deviation from anti-alignment.

Nonetheless, the phases contain important information, and in certain circumstances they *can* help break the degeneracy between mass and eccentricity. For ease of discussion, we first define

$$\phi_{\text{ttv}} \equiv \angle(V \times \text{sgn}\Delta) \quad (16)$$

$$\phi'_{\text{ttv}} \equiv \angle(V' \times \text{sgn}\Delta), \quad (17)$$

where  $\text{sgn}\Delta = 1$  if  $\Delta > 0$ , and  $-1$  otherwise. With these definitions,  $\phi_{\text{ttv}} = 0$  and  $\phi'_{\text{ttv}} = 180^\circ$  when  $Z_{\text{free}} = 0$ , independent of the sign of  $\Delta$ . Note that if  $\phi_{\text{ttv}} = 0$ , then  $\delta t$  crosses zero from above to below whenever the longitude of conjunctions points along the line of sight (regardless of the sign of  $\Delta$ ); similarly, if  $\phi'_{\text{ttv}} = 180^\circ$ ,  $\delta t'$  crosses zero from below when  $\lambda^j = 0$ . We consider the two possibilities:

- If the observed TTV’s have a phase shift with respect to  $\lambda^j$ , that directly implies that free eccentricities are present. A large phase shift implies  $|Z_{\text{free}}| \gtrsim |\Delta|$ .
- If there is no phase shift (i.e.,  $\phi_{\text{ttv}} = 0$  and  $\phi'_{\text{ttv}} = 180^\circ$ ), that does not necessarily imply that  $|Z_{\text{free}}| = 0$ . Instead,  $|Z_{\text{free}}|$  could be large but the phase of  $Z_{\text{free}}$  vanishes. However, such a coincidence is unlikely. Even if the phase of  $Z_{\text{free}}$  vanished initially, secular precession would operate on the timescale  $\sim P/\mu$  to randomize the phase. So if the free eccentricity is large ( $|Z_{\text{free}}| \gg |\Delta|$ ), TTV phases should be randomly distributed between 0 and  $2\pi$ . Conversely, if  $|Z_{\text{free}}| \lesssim |\Delta|$ , phase shifts should be small. If many of the systems observed by Kepler have zero or near zero phase shifts, one could argue that most of them have small free eccentricities ( $|Z_{\text{free}}| \lesssim |\Delta|$ ). Such a result, if found

vided the complex phase of  $Z_{\text{free}}$  is very nearly 0 or  $\pi$  (depending on the sign of  $\Delta$ ). However, as we argue below, such a coincidence would be rare (Fig. 10).

<sup>5</sup> Recall that we define the phases ( $\angle V$  and  $\angle V'$ ) to be relative to the time when the longitude of conjunctions points along the line of sight ( $\lambda^j = 0$ ). With this definition, the phases can be determined from observed TTV signals with no ambiguity about the origin of time or angle.

true (see Section 3), has interesting implication for the dynamical history of these planets. Moreover, for the task at hand, it would break the degeneracy in the mass determination: when  $|z_{\text{free}}/\Delta|$  is negligible in Eqs. (8)–(9),  $\mu$  and  $\mu'$  are directly determined by the two TTV amplitudes.

Our above discussion is greatly aided by the analytical expressions. Using N-body simulations alone, it is difficult to elucidate the degeneracy between mass and free eccentricity. Moreover, the fact that TTV phases contain important information has hitherto been overlooked, only becoming transparent with the analytical formulae.

We conclude this subsection by comparing with previous work. Agol et al. (2005) estimate the TTV amplitudes for two near-resonant planets, assuming that the planets' initial orbits are circular. In that case,  $z_{\text{free}} = -z_{\text{forced}}$  initially, and hence  $Z_{\text{free}} \sim \mu/\Delta$  (Eq. 13). Equations (14)–(15) then imply  $|V| \sim P(\mu/|\Delta|)(1 + \mu/|\Delta|^2)$ , in agreement with Equations (29)–(31) of Agol et al. (2005) in the two corresponding limits ( $|\Delta|^2/\mu \ll 1$  and  $\gg 1$ ). We note, though, that there is little reason why the initial orbits should be circular. If the planets suffer weak damping (e.g., by tides or a disk), that would tend to damp away the free eccentricities, but the forced eccentricities would remain intact as long as proximity to resonance is maintained. Agol et al. (2005) also derive analytically an expression for the TTV that is valid when  $Z_{\text{free}} = 0$  (see their Appendix). Nesvorný & Morbidelli (2008) and Nesvorný (2009) derive a general analytic expression for the TTV, but their expressions have not been applied to Kepler planets due to their algebraic complexity, which arises partly because they do not distinguish free from forced eccentricities.

### 2.3. Testing with N-body Simulations

We test our TTV expressions with N-body simulations, choosing cases that illustrate our discussion above. Figure 2 shows transit time variations from two separate N-body simulations for a pair of planets that resemble Kepler-18 c/d, showing agreement with the predictions of Equations (1)–(10). In the top panel the planets have zero free eccentricity and hence TTV are in phase with  $\lambda^j$ , while in the bottom panel the inner planet has a free eccentricity and hence the signals are not in phase. Numerically, we reach the state of zero free eccentricity by first weakly damping the planets' velocities to the local circular speed over a few million orbits. Many other forms of weak damping will also remove free eccentricities.

Figure 3 illustrates the degeneracies inherent in extracting planet parameters from TTV, and how these can be partially removed with the phase information, as discussed in Section 2.2. In the top panel, we perform a simulation similar to the one in the top panel of Figure 2, with the same periods for the two planets, but in this case the masses of the two planets are reduced by factors of 0.2 and 0.37. Furthermore, after the free eccentricities are damped away the two planets' complex eccentricities are increased by  $z_{\text{free}} = z'_{\text{free}} = 0.05$ . The resulting TTV's are almost identical to those in the top panel of Figure 2, despite the vastly different parameters. Hence if one observed such TTV's, one could not determine the

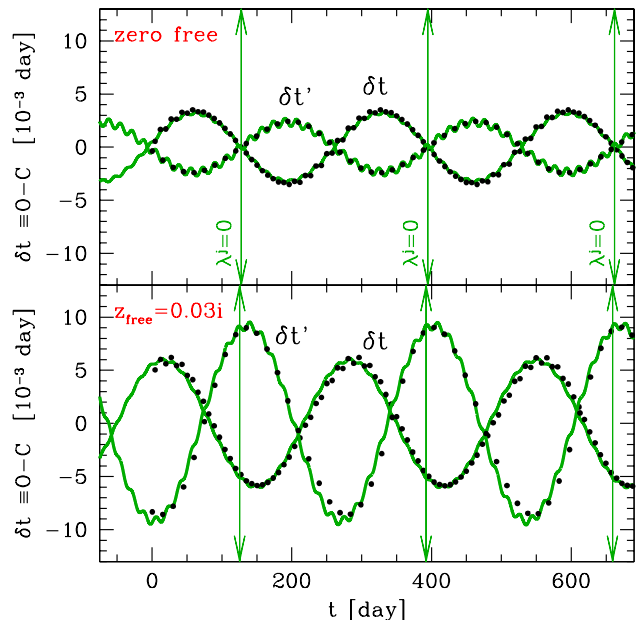


FIG. 2.— TTV's of a near-resonant planet pair, without (above) and with (below) free eccentricity. Planet periods and masses are chosen to be close to those of Kepler-18c/d (see Table 1) with  $\Delta = -0.028$  relative to the 2:1 resonance. The black points show the N-body simulated TTV signals for the two planets and the green curves the analytic expressions (Eqs. 1–10). The vertical arrows show the times at which the longitude of conjunctions points at the observer ( $\lambda^j = 0$ ). The duration between two such arrows is the super-period. In the top panel, the pair have zero free eccentricities, so their TTV cross through zero when  $\lambda^j = 0$ , with the inner planet crossing from above, and the outer from below. The bottom panel shows the case when the inner planet has free eccentricity  $z_{\text{free}} = 0.03i$ , which is  $\sim 20$  times greater in amplitude than its forced eccentricity and is of order  $|\Delta|$ . In this case, the TTV's are no longer in phase with  $\lambda^j$ , though the inner and outer TTV's are still anti-correlated. The small rapid wiggles in the green curves are due to our inclusion of the 3:2 forcing term in addition to the 2:1; this clearly has little effect.

planets' masses. Nonetheless, the fact that the TTV's are in phase with  $\lambda^j$  in the top panel of Figure 3 is due to our judicious choice of  $\angle z_{\text{free}} = \angle z'_{\text{free}} = 0$ . Even though they are initially in phase, this cannot remain true for long: the black points in the bottom panel show the TTV's in the same simulation, but  $10^6$  days later, by which time the two planets' free longitudes of periapse have precessed by  $\sim 70^\circ$ . As a result, the TTV's are no longer in phase with  $\lambda^j$ . By contrast, the TTV's of pairs with zero free eccentricity would always remain in phase with the longitude of conjunction (faint green line in bottom panel of Fig. 3). This example shows that if many systems are observed to have small TTV phase shifts, one could argue that most planetary systems likely have small free eccentricities, although one cannot be certain for any particular system. Furthermore, if the free eccentricities are small, one could determine planet masses from TTV data (see Fig. 10).

### 3. APPLYING TO KEPLER PAIRS: MASS AND FREE ECCENTRICITY

Equations (8)–(9) show clearly how planet mass and eccentricity affect the TTV signals. The task to invert observed TTV signals to obtain physical parameters is now almost trivial.

Transit times have been published for 13 Kepler sys-

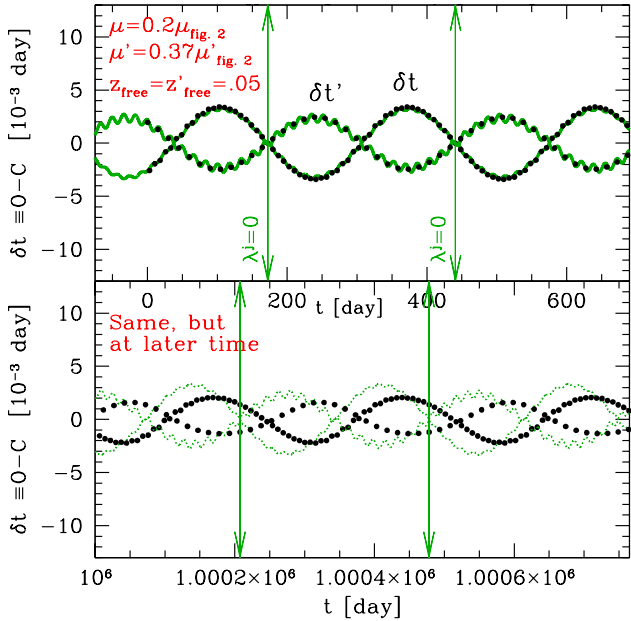


FIG. 3.— Degeneracies in extracting planet parameters using TTV signals. Here points result from N-body simulations, and green curves are theoretical results. The top panel shows a pair of planets exhibiting the same TTV signals as those in the top panel of Fig. 2, but the ones here have reduced planet masses and non-zero free eccentricities (as marked). The TTV’s remain in phase with  $\lambda^j$  because we deliberately chose free eccentricities with  $\lambda_{z_{\text{free}}} = \lambda_{z'_{\text{free}}} = 0$  initially. This panel illustrates that TTV measurements alone do not allow unique inference of mass and free eccentricity. Additional constraints must be imposed. The points in the bottom panel show the same system but  $10^6$  days later, when the phases of the free eccentricities have secularly precessed. The TTV’s are no longer in phase with  $\lambda^j$ . The faint green curves in this panel are what the TTV’s would look like for the system with zero free eccentricity (i.e., the system in the top panel of Fig. 2) – its TTV remains in phase. Therefore the phase of the TTV provides a statistical way to break the degeneracies inherent in the TTV’s.

tems with confirmed planets (e.g., Cochran et al. 2011; Fabrycky et al. 2012b; Ford et al. 2012). Here, we apply our formula to those near 2:1 or 3:2 resonances. We further restrict to systems that have gone through at least one complete TTV cycle, leaving us with 6 systems, all of which have inner period  $< 10$  days.

Our results are depicted in Figures 4–9 and Tables 1–2. All six short period systems appear consistent with having small free eccentricity  $|Z_{\text{free}}| \lesssim 0.01$ , with three of them consistent with zero free eccentricity. Before discussing these results, we describe our method.

### 3.1. Extracting the Complex TTV

Given a sequence of transit times for two planets in a system, we obtain the parameters  $P, P', T, T', V, V'$  in Equations (1)–(4) as follows. We write the transit times for the inner planet as (Eq. 1)

$$t_{\text{trans}} = T + P i_{\text{trans}} + \text{Real}(V) \sin \lambda^j + \text{Imag}(V) \cos \lambda^j \quad (18)$$

where  $i_{\text{trans}} = 0, 1, \dots$  is the transit number. Since  $|V| \ll P$ , we proceed in two steps. First, we fit the inner planet’s  $t_{\text{trans}}$  vs.  $i_{\text{trans}}$  with a straight line, thereby extracting  $P$  and  $T$ , and also do the same for the outer planet, extracting  $P', T'$ . Our fits are done by linear least squares (e.g. Press et al. 1992). Second, we fit for the four parameters explicit in Equation (18) (i.e.,

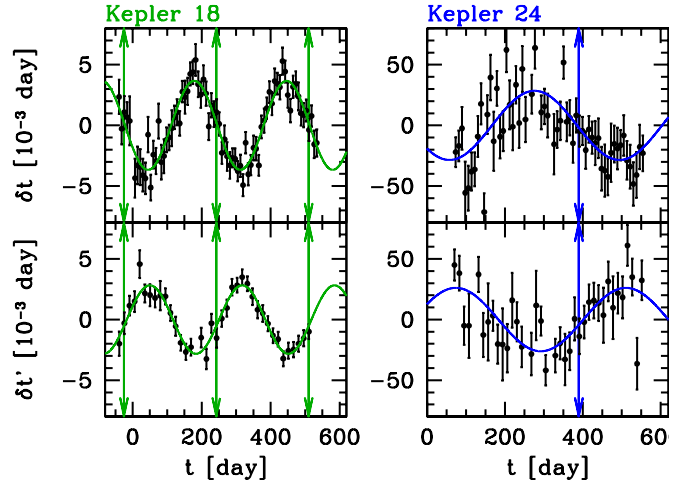


FIG. 4.— TTV data (black points with errorbars), best-fit theoretical curve, and times when the longitude of conjunction points at the observer, i.e.,  $\lambda^j = 0$  (vertical arrows). These two systems have near-zero phase shift, as evidenced by the fact that the inner planet’s TTV (upper panel) crosses through zero from above at times when  $\lambda^j = 0$ ; and the outer planet’s TTV crosses through zero from below. Hence these systems likely have zero free eccentricity. Kepler 18 data from Cochran et al. (2011), and Kepler 24 data from Ford et al. (2012). The former system lies inside the 2:1 resonance, while the latter one lies outside the 3:2.

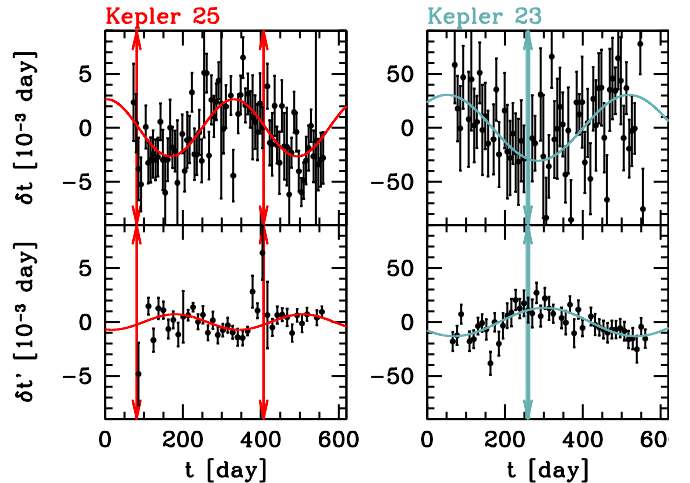


FIG. 5.— TTV data and fits. Similar to Figure 4 but for Kepler 25 (data from Steffen et al. 2012)) and Kepler-23 (data from Ford et al. 2012). Kepler 25 has zero phase shift, but Kepler 23 has a non-zero phase shift.

$T, P, \text{Real}(V), \text{Imag}(V)$ ) using a second least squares fit for the inner planet’s transit times; in this fit,  $\lambda^j$  is determined by Equations (3)–(4) at times  $t_{\text{trans}}$ , where the parameters  $T, P, T', P'$  are the ones obtained from the first fits. This refitting for  $P$  helps to remove the small linear trend that remains after the first fit. We repeat for the outer planet. This procedure implicitly assumes that the period of the TTV curve is the super-period (Eq. 5). That this assumption is valid for the six Kepler pairs of interest can be seen by comparing the fit to the data (Figures 4–6). The results of the fits are listed in Table 1.

To obtain error estimates for the best-fit values, we use the covariance matrix provided by the second least-



TABLE 1  
COMPLEX TTV FOR SIX KEPLER SYSTEMS

Kepler ID	j:j-1	$P$ [d]	$P'$ [d]	$\Delta$	$ V $ [d]	$\phi_{\text{ttv}}$	$ V' $ [d]	$\phi'_{\text{ttv}}$	$\chi^2_{\text{dof}}$	$\chi'^2_{\text{dof}}$
18c/d	2:1	7.642	14.86	-0.028	0.0037( $\pm 7\%$ )	$-4.3^\circ \pm 4^\circ$	0.0028( $\pm 10\%$ )	$169^\circ \pm 5^\circ$	0.95	0.71
24b/c	3:2	8.146	12.33	0.0094	0.028( $\pm 20\%$ )	$-3.9^\circ \pm 12^\circ$	0.026( $\pm 20\%$ )	$180^\circ \pm 16^\circ$	1.95	1.28
25b/c	2:1	6.239	12.72	0.0195	0.0026( $\pm 20\%$ )	$5.7^\circ \pm 12^\circ$	0.00072( $\pm 30\%$ )	$200^\circ \pm 22^\circ$	1.19	1.60
23b/c	3:2	7.107	10.74	0.0077	0.031( $\pm 40\%$ )	$-68^\circ \pm 18^\circ$	0.013( $\pm 30\%$ )	$120^\circ \pm 17^\circ$	1.88	0.93
28b/c	3:2	5.912	8.986	0.013	0.0082( $\pm 20\%$ )	$-50^\circ \pm 14^\circ$	0.0086( $\pm 30\%$ )	$130^\circ \pm 16^\circ$	0.87	3.43
32b/c	3:2	5.901	8.752	-0.011	0.0062( $\pm 30\%$ )	$45^\circ \pm 15^\circ$	0.0077( $\pm 30\%$ )	$228^\circ \pm 19^\circ$	1.33	2.60

NOTE. — Columns labelled  $|V|$ ,  $\phi_{\text{ttv}}$ ,  $|V'|$ , and  $\phi'_{\text{ttv}}$  are the amplitudes and phases of the complex TTV, extracted from the transit times with a least squares fit (see text); the phases are defined in Equations (16)–(17). The last two columns are the values of  $\chi^2/(\text{deg. of freedom})$  from the fits for the inner and outer planet. The phases for the first three systems in the table are consistent with zero free eccentricity ( $\phi_{\text{ttv}} = 0$ ,  $\phi'_{\text{ttv}} = 180^\circ$ ), and those of the latter three are not. Errors on the TTV amplitudes and phases are at 68% confidence.

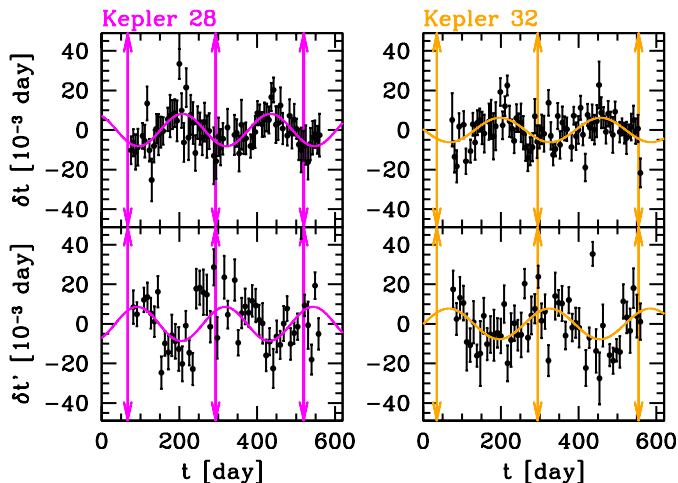


FIG. 6.— TTV data and fits for Kepler-28 (data from Steffen et al. 2012) and Kepler-32 (data from Fabrycky et al. 2012a). Both these systems have non-zero phase shifts.

TABLE 2  
PLANET MASSES

Kepler ID	analytical Mass [ $M_\oplus$ ]		N-body Mass [ $M_\oplus$ ]	
	$m_{\text{nominal}}$	$m'_{\text{nominal}}$	$m$	$m'$
18c/d	$20.2 \pm 1.9$	$17.4 \pm 1.2$	$17.3 \pm 1.7$	$15.8 \pm 1.3$
24b/c	$28.4 \pm 5.9$	$50.4 \pm 7.9$	$56.1 \pm 15.8$	$102.8 \pm 21.4$
25b/c	$7.13 \pm 2.5$	$13.1 \pm 2.6$	$8.1 \pm 3.1$	$13.3 \pm 3.9$
23b/c	$14.7 \pm 3.8$	$55 \pm 22$	$4.8 \pm 15.6$	$15.0 \pm 49.8$
28b/c	$14.8 \pm 4.2$	$22.9 \pm 5.6$	$3.8 \pm 6.9$	$4.9 \pm 9.3$
32b/c	$6.0 \pm 1.9$	$7.59 \pm 2.0$	$7.2 \pm 4.1$	$5.2 \pm 3.5$

NOTE. — The nominal masses  $m_{\text{nominal}}$  and  $m'_{\text{nominal}}$  are calculated using Equations (19)–(20); these are likely modest overestimates of the true masses. For the stellar masses, and the N-body determined planet masses, we use those listed in Table 5 of Fabrycky et al. (2012a), except for Kepler-18 for which we use values from Cochran et al. (2011).

square fit and assume that the quoted 1- $\sigma$  errors in the transit time data are independent and Gaussian. The errors in periods ( $P, P'$ ) and fiducial transit times ( $T, T'$ ) are negligibly small (fractional error  $\ll 10^{-4}$ ). All of our errors are quoted at 68% confidence.

Figure 7 depicts the inferred values of  $V$  and  $V'$  for the twelve planets. Figure 8, which plots just the phases, summarizes the main result of our analysis: three of

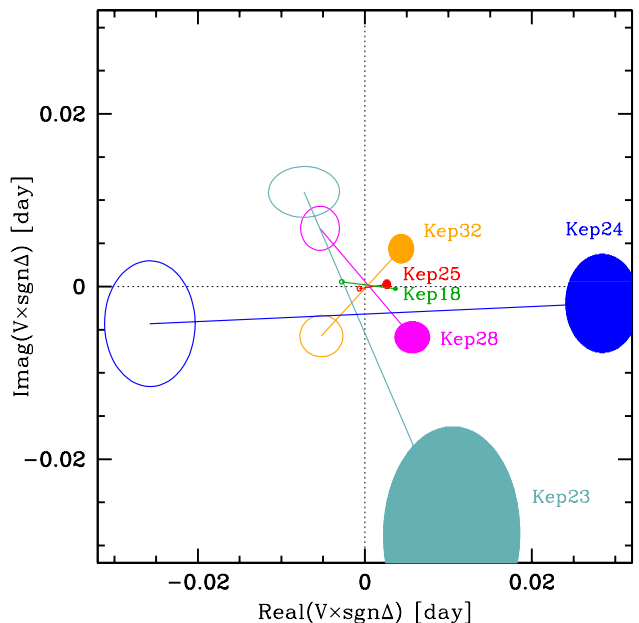


FIG. 7.— Best-fit complex TTVs, plotted in the complex plane. Here,  $\text{sgn}\Delta$  stands for the sign of  $\Delta$  – this term is included so that pairs with zero free eccentricity would lie on the horizontal dotted line with the inner planet to the right, regardless of the sign of  $\Delta$ . The filled ellipses are the 68% confidence regions for the inner planet of each pair ( $V$ ), and the open ellipses are for the outer planet ( $V'$ ), connected here as dumbbells. Kepler 18, 24, and 25 are all consistent with having zero free eccentricities, while three other systems shown here are discrepant (Kepler 23, 28, 32). But even for these, the inner planets still lie mostly to the right suggesting that the free eccentricity is small ( $|Z_{\text{free}}| \lesssim |\Delta|$ ).

the systems are consistent with having zero phase and three are not. But all six systems have  $|\phi_{\text{ttv}}| \lesssim 90^\circ$ . This strongly suggests that  $|Z_{\text{free}}| \lesssim |\Delta| \sim 0.01$ ; otherwise, the six systems would have random phases between  $-180^\circ$  and  $180^\circ$ .

Table 2 lists the masses that would be inferred by setting  $Z_{\text{free}} = 0$  in Equations (8)–(9), i.e.,

$$m_{\text{nominal}} \equiv M_* \left| \frac{V' \Delta}{P' g} \right| \pi j \quad (19)$$

$$m'_{\text{nominal}} \equiv M_* \left| \frac{V \Delta}{P f} \right| \pi j^{2/3} (j-1)^{1/3}. \quad (20)$$

Figure 9 displays these nominal masses versus planet

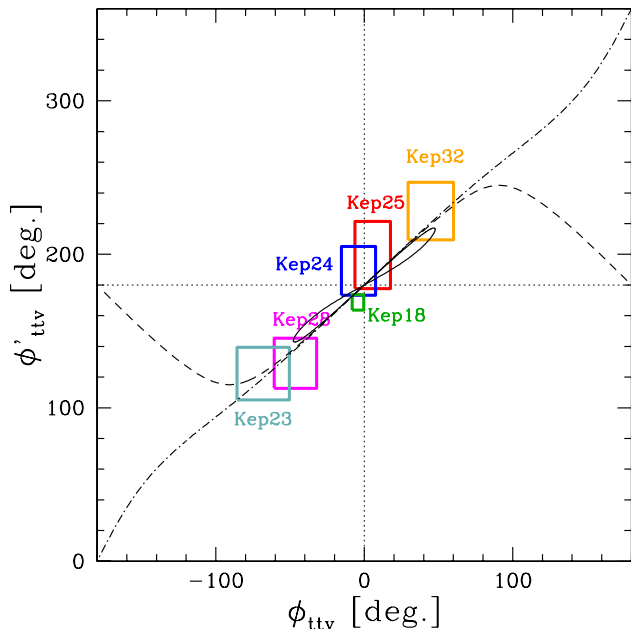


FIG. 8.— Phases of the complex TTV. The x-axis is the phase of the inner planet’s TTV, and the y-axis is for the outer planet (Eqs. 16–17). A system with zero free eccentricity would lie at the center of the plot. The width and height of each rectangle denote the 68% confidence limits measured from Kepler data for the 6 systems in this study. The three curves represent the theoretical prediction for the TTV phases when  $|Z_{\text{free}}| = \Delta$  (solid curve),  $|Z_{\text{free}}| = 1.5\Delta$  (dashed curve) and  $|Z_{\text{free}}| = 2\Delta$  (dot-dashed curve) for systems near the 3:2 resonance. It appears that all systems can be explained with small free eccentricity,  $|Z_{\text{free}}| \lesssim |\Delta|$ .

radii. The true mass is related to the nominal mass by

$$\frac{m}{m_{\text{nominal}}} = \frac{1}{|1 - Z_{\text{free}}/(2g\Delta/3)|}, \quad (21)$$

and similarly for the outer planet after replacing  $g \rightarrow -f$ . Although  $Z_{\text{free}}$  is not known, the inference that  $|Z_{\text{free}}| \lesssim |\Delta|$  implies that the nominal masses are typically close to, but a little bigger than, the planets’ true masses (Section 3.4).

### 3.2. Systems with negligible TTV phase shift: Kepler-18, 24, 25

From Figures 4–5, we see that Kepler 18, 24, and 25 all have very small phase shifts:  $\delta t$  crosses through zero from above at the times when  $\lambda^j = 0$ , and  $\delta t'$  crosses from below. This can also be seen in Figures 7–8.

**Kepler 18:** This system has currently one of the best measured TTV, and its TTV phase lies very close to zero. If we *assume* that this system has zero free eccentricity, then we may deduce the masses of the two planets with small error bars. These values lie close to those obtained using an N-body fit (Table 2).

But to obtain these mass estimates and small error bars, we must assume that the free eccentricities vanish (or  $|Z_{\text{free}}| \ll |\Delta|$ ). Without this assumption, the masses of the planets are degenerate with the free eccentricity: one could choose an infinite sequence of  $Z_{\text{free}}$  with  $\angle Z_{\text{free}} \approx 0$  or  $\pi$  to reproduce Kepler 18’s TTV signals, each corresponding to a different set of masses. However, the secular precession of  $Z_{\text{free}}$  implies that a specially aligned  $Z_{\text{free}}$  would be unlikely. It is far more likely the free eccentricities are very small,  $|Z_{\text{free}}| \lesssim |\Delta| \sim 0.03$ .

Without explicitly assuming that the free eccentricity is small, Cochran et al. (2011) obtain mass estimates and errors similar to ours by fitting the TTV signal (alone) with N-body simulations (Table 2). We suggest this result is fortuitous: their N-body simulations have not exhaustively searched all possible mass-eccentricity combinations. Nearly the same TTV signals can be produced by much lower planet masses, as can be seen by comparing the top panels of Figures 2 and 3. In truth, the TTV’s in those two panels differ slightly. Such “chopping” (Holman et al. 2010; Fabrycky et al. 2012a) or other non-sinusoidal behavior might be used to break the degeneracy between mass and eccentricity. But it is not clear if the data is of high enough quality to distinguish the difference between those two panels. By contrast, in Kepler 36 for example, which lies close to a high  $j$  resonance (7:6), the TTV signals are significantly non-sinusoidal, and that likely allowed the N-body fit to break the degeneracy (Carter et al. 2012).

In the case of Kepler 18, additional non-TTV information, such as radial velocity measurements and theoretical expectations for planet density allow one to eliminate most of the solutions. But that would not be possible for most systems. This example accentuates the importance of an analytical understanding: the degeneracy between mass and eccentricity are explicit in the formula.

**Kepler 25:** The TTV phases of Kepler 25b/c are also consistent with zero, a strong indication that the planets’ free eccentricities are very small. From our fits for  $|V|$  and  $|V'|$  listed in Table 1, we derive nominal masses for the planets as listed in Table 2. These are likely close to the true planet masses. They are consistent with those from N-body fits (Table 2). However, as for the Kepler-18 case, the N-body fit without any assumption on the value of the free eccentricity is incomplete. An alternative solution that matches the observations is, e.g., inner and outer masses of  $0.59M_{\oplus}$ ,  $3.0M_{\oplus}$  and  $Z_{\text{free}} = -0.05$ .

**Kepler 24:** Similar arguments apply to Kepler 24, for which the phases are also consistent with zero. We derive masses of  $28.4 \pm 5.9M_{\oplus}$  and  $50.4 \pm 7.9M_{\oplus}$  for the inner and outer planets, when we assume that the free eccentricity vanishes. Fabrycky et al. (2012a) list masses from N-body fits of  $56.1 \pm 15.8M_{\oplus}$  and  $102.8 \pm 21.4M_{\oplus}$ , and large eccentricities, of order 0.4 and 0.3 for the inner and outer planets. However, the TTV signal suggests smaller eccentricities.<sup>6</sup>

With planet radii of 2.4 and  $2.8R_{\oplus}$  (Ford et al. 2012; Batalha et al. 2012), our nominal masses imply surprisingly high densities of  $\sim 12\text{g/cm}^3$ , comparable to the density of lead (Fig. 9). But the true masses and densities could be smaller than these nominal values by a factor of  $\sim 2$  if the free eccentricities were  $\sim 0.01$ , even

<sup>6</sup> The solution of Fabrycky et al. (2012a) for Kepler 24 yields  $|Z_{\text{free}}| \ll e$ : their eccentricity vectors nearly cancel in the combination  $fz + gz'$ . That is likely why their masses are only twice as large as ours rather than  $\sim e/|\Delta| \sim 20$  times larger. We note also that the TTV super-period from the periods in Table 1 ( $P^j \sim 450$  d) agrees with that of Ford et al. (2012), but disagrees with that from Table 6 in Fabrycky et al. (2012a) by 60% because the latter uses osculating periods (D. Fabrycky, personal communication). Ford et al. (2012) report two more candidates in the system, KOI-1102.04 and KOI-1102.03. If real (they are absent from the table in Batalha et al. 2012), they are near resonant with the two planets here but with  $\Delta \sim 3\%$  or  $4\%$ , respectively. These should not significantly affect the TTV amplitude.

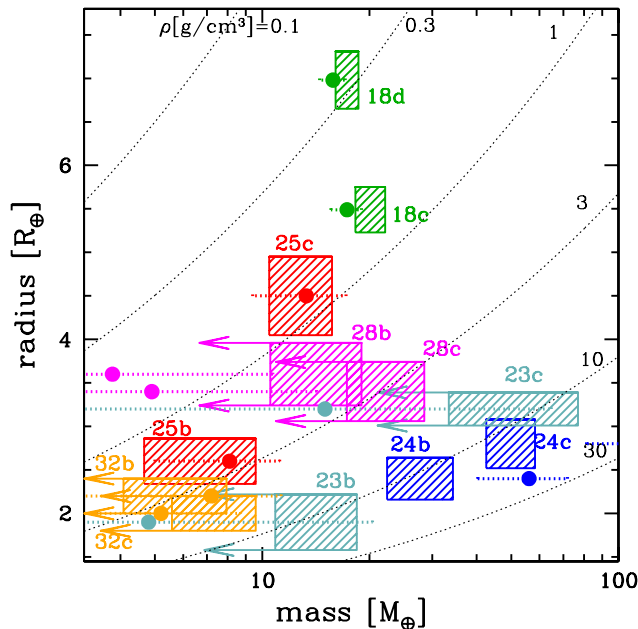


FIG. 9.— Nominal mass vs. radius for planets in the 6 Kepler systems we examine: The shaded rectangles show our values for the nominal masses (Eqs. 19–20), plotted against planet radii, encompassing our error estimates. The nominal masses are likely modest overestimates of the true masses, by a factor of 1–2 (Fig. 10). For comparison, masses determined in the literature with N-body simulations are marked with filled circles. For radii, see references in Figs. 4–6. The error estimates on radii are unpublished for Kepler 24, 25, 23, and 28, and hence assumed to be 10% for this plot.

though in that case it would have to be a coincidence that the phase nearly vanishes.

### 3.3. Systems with TTV phase shift: Kepler-23,28,32

Three out of six systems we analyze are inconsistent with zero free eccentricity: their TTV phases differ significantly from  $\phi_{\text{ttv}} = 0$  and  $\phi'_{\text{ttv}} = 180^\circ$ . All are near 3:2 resonances. Planet masses in these cases cannot be reliably determined. However, as is apparent from Fig. 8, there is an absence of systems with large phase shifts.

**Kepler 23:** This pair has the largest phase shift,  $\sim 70^\circ$ . The nominal masses correspond to high planet densities  $\sim 10\text{g/cm}^3$ , comparable to silver. Equation (21) shows that if one takes  $|Z_{\text{free}}| = 4\Delta = 0.03$ , for instance, then the real masses would be three times lower than the nominal ones.

**Kepler 28 and 32:** The nominal masses in these two cases yield planet densities  $\sim 3\text{g/cm}^3$ . The true masses are likely smaller (Eq. 21). However, if the collective behavior of these TTV pairs indeed implies that  $|Z_{\text{free}}| \approx |\Delta|$ , then the true masses lie close to the nominal ones.

### 3.4. Extracting Mass and Eccentricity

Given the measured TTV phases and nominal masses (Figs. 8 and 9), what can be concluded about the planets' eccentricities and masses? As emphasized above, the mass-eccentricity degeneracy can only be broken in a statistical way. Because of the small number of systems analyzed in this paper, we leave a proper statistical study to future work. Instead, here we model our results by assuming that the free eccentricities of all planets are randomly drawn from a Rayleigh distribution (Binney & Tremaine 2008) with random phases, i.e., that the real

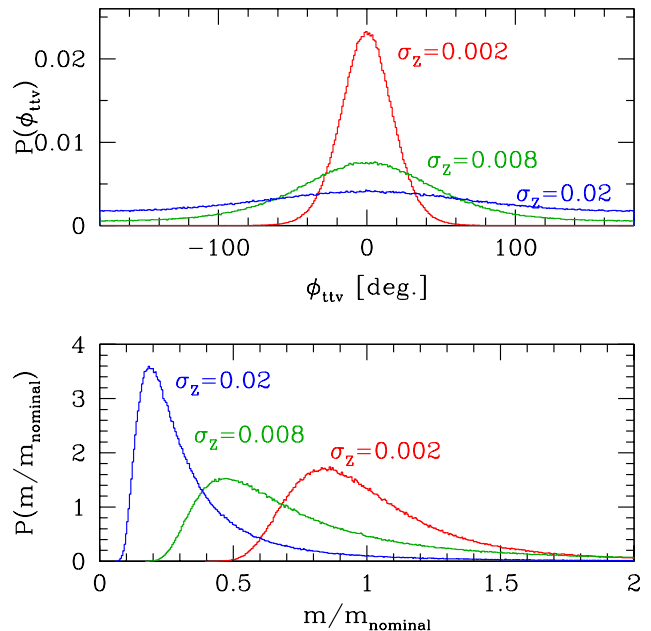


FIG. 10.— Probability distributions of TTV phase and true planet mass, assuming that the real and imaginary parts of  $Z_{\text{free}}$  are independent Gaussians, with r.m.s.  $\sigma_Z$ . The top panel shows the resulting distributions of TTV phases (via Eq. 8) for three values of  $\sigma_Z$ , after taking  $|\Delta f 2/3| = 0.008$ ; equivalently, the three distributions have  $\sigma_Z/|\Delta f 2/3| = 0.3, 1,$  and  $3$ . The bottom panel shows the resulting distributions of  $m/m_{\text{nominal}}$  (via Eq. 21).

and imaginary parts of the complex free eccentricities ( $z_{\text{free}} \equiv e_x + ie_y$ ) are drawn from independent Gaussians

$$P(e_x) = \frac{1}{\sqrt{2\pi}\sigma} \exp\left(-\frac{e_x^2}{2\sigma^2}\right), \quad (22)$$

and  $e_y$  similarly. The top panel of Figure 10 shows the resulting phase distribution for three values  $\sigma_Z = \sigma\sqrt{f^2 + g^2}$  (assuming  $f\Delta$  is fixed). From the fact that half of the systems have phases  $|\phi_{\text{ttv}}| \lesssim 10^\circ$ , we infer that  $\sigma_Z \sim 0.002 - 0.008$ . Therefore the free eccentricities of the planets are quite small,  $\lesssim 0.006$ . The bottom panel of Figure 10 shows the distribution of the ratio of true to nominal mass (Eq. 21). For the inferred  $\sigma_Z$ , we see that the true masses are comparable to the nominal masses, within around a factor of 2. We emphasize, however, that it is not necessarily the case that the free eccentricities in these six systems are drawn from the same distribution. Instead, it could be that the three systems consistent with zero phase all have precisely  $Z_{\text{free}} = 0$ . In that case, the nominal masses for those systems would be their true masses. A better assessment of probable values awaits future data analysis.

## 4. SUMMARY

### 4.1. Analytical TTV

We have derived simple analytical expressions for the TTV from two planets near a first order mean motion resonance (Eqs. 1–10). These show that the amplitude and phase of the TTV depend on both planet mass and free eccentricity. There is an inherent degeneracy between mass and free eccentricity which in general prevents either from being determined independently of the other. This degeneracy, however, may be (partially) broken under certain circumstances, based on probability



arguments.

There is a special moment in time when the longitude of conjunction points along the line of sight. If the phase of TTV is zero relative to this time, then it is likely that the free eccentricity in the system is zero. Moreover, if the free eccentricity is zero, the TTV amplitudes can be used to uniquely determine planet masses.

When applying this technique to six published systems, we find that three of them are consistent with zero TTV phase, while the other three deviate by less than a radian. This clustering around zero phase can be most naturally explained if all systems have free eccentricity of order a percent or less—which is comparable to the typical distance to resonance in these systems. Furthermore, because the free eccentricities are small, the nominal masses determined by TTV are likely close to the true masses, within a factor  $\lesssim 2$ .

Without the analytical TTV expressions and relying only on N-body simulations, it would be hard to reach these conclusions.

#### 4.2. Implications of Small Free Eccentricities

The very small free eccentricities suggest that these planets have experienced damping, as suggested also by the resonant repulsion theory (Lithwick & Wu 2012, see also Batygin & Morbidelli 2012). In that work, we found that if Kepler planets have experienced substantial energy dissipation, but substantially less angular momentum damping, the two planets will be repelled from each other. This would explain the observed pile-up of planets just wide of resonances. A corollary of this theory is that low mass planets in the Kepler sample should have little if any free eccentricity.

Although this appears to be confirmed by three of the six systems we analyze, we are puzzled by the small but finite free eccentricities in the other three systems. Assuming that resonant repulsion indeed occurred, it would require that the planets' eccentricities were subsequently excited, perhaps by interplanetary interactions. Such a scenario would argue against tides as the mechanism

of dissipation causing resonant repulsion, because tides would have to act over very long times to be effective. Instead, dissipation by a disk of gas or planetesimals are more plausible damping agents.

TTV data have also been reported for Kepler 9b/c and Kepler 30b/c (Holman et al. 2010; Fabrycky et al. 2012a). These pairs contain one or two giant planets. We find preliminary evidence that these systems have large TTV phases. This, if true, will indicate the presence of large free eccentricities in systems of giant planets, in contrast to the lower mass planets discussed here. We are currently analyzing Kepler public lightcurve data to distill more TTV systems. One interesting issue to pursue is whether planet pairs at much shorter or much longer orbital periods have the same characteristics as those analyzed here.

Many planet pairs are also near resonance with a third planet. This may bring further complications to our TTV analysis but is not considered here.

#### 4.3. Values of Planet Masses

All six systems we analyze have orbital periods between 6 and 15 days, and planet radii ranging from 2 to  $7R_{\oplus}$ . We confirm the mass estimates of Cochran et al. (2011) for Kepler 18c/d, and the mass estimates of Fabrycky et al. (2012a) for Kepler 25b/c, under the assumption that these systems have  $|Z_{\text{free}}| \lesssim |\Delta|$ , consistent with their small phase. Densities of these planets range between 0.3 and  $2\text{g/cm}^3$ . For Kepler 28b/c, 32b/c, we obtain nominal mass upper limits that lead to density upper limits of  $\sim 3\text{g/cm}^3$ . We also argue that these upper limits are likely not too different from the real masses. For Kepler 24b/c and 23b/c, the nominal densities are  $\sim 10\text{g/cm}^3$ .

Y.L. acknowledges support from NSF grant AST-1109776. JWX and YW acknowledge support by NSERC and the Ontario government. We thank the referee, Dan Fabrycky, for a helpful report.

#### REFERENCES

- Agol, E., Steffen, J., Sari, R., & Clarkson, W. 2005, MNRAS, 359, 567
- Batalha, N. M., Rowe, J. F., Bryson, S. T., Barclay, T., Burke, C. J., Caldwell, D. A., Christiansen, J. L., Mullally, F., Thompson, S. E., Brown, T. M., Dupree, A. K., Fabrycky, D. C., Ford, E. B., Fortney, J. J., Gilliland, R. L., Isaacson, H., Latham, D. W., Marcy, G. W., Quinn, S., Ragozzine, D., Shporer, A., Borucki, W. J., Ciardi, D. R., Gautier, III, T. N., Haas, M. R., Jenkins, J. M., Koch, D. G., Lissauer, J. J., Rapin, W., Basri, G. S., Boss, A. P., Buchhave, L. A., Charbonneau, D., Christensen-Dalsgaard, J., Clarke, B. D., Cochran, W. D., Demory, B.-O., Devore, E., Esquerdo, G. A., Everett, M., Fressin, F., Geary, J. C., Girouard, F. R., Gould, A., Hall, J. R., Holman, M. J., Howard, A. W., Howell, S. B., Ibrahim, K. A., Kinemuchi, K., Kjeldsen, H., Klaus, T. C., Li, J., Lucas, P. W., Morris, R. L., Prsa, A., Quintana, E., Sanderfer, D. T., Sasselov, D., Seader, S. E., Smith, J. C., Steffen, J. H., Still, M., Stumpe, M. C., Tarter, J. C., Tenenbaum, P., Torres, G., Twicken, J. D., Uddin, K., Van Cleve, J., Walkowicz, L., & Welsh, W. F. 2012, ArXiv e-prints
- Batygin, K. & Morbidelli, A. 2012, ArXiv e-prints
- Binney, J. & Tremaine, S. 2008, Galactic Dynamics: Second Edition (Princeton University Press)
- Carter, J. A., Agol, E., Chaplin, W. J., Basu, S., Bedding, T. R., Buchhave, L. A., Christensen-Dalsgaard, J., Deck, K. M., Elsworth, Y., Fabrycky, D. C., Ford, E. B., Fortney, J. J., Hale, S. J., Handberg, R., Hekker, S., Holman, M. J., Huber, D., Karoff, C., Kawaler, S. D., Kjeldsen, H., Lissauer, J. J., Lopez, E. D., Lund, M. N., Lundkvist, M., Metcalfe, T. S., Miglio, A., Rogers, L. A., Stello, D., Borucki, W. J., Bryson, S., Christiansen, J. L., Cochran, W. D., Geary, J. C., Gilliland, R. L., Haas, M. R., Hall, J., Howard, A. W., Jenkins, J. M., Klaus, T., Koch, D. G., Latham, D. W., MacQueen, P. J., Sasselov, D., Steffen, J. H., Twicken, J. D., & Winn, J. N. 2012, Science, 337, 556
- Cochran, W. D., Fabrycky, D. C., Torres, G., Fressin, F., Désert, J.-M., Ragozzine, D., Sasselov, D., Fortney, J. J., Rowe, J. F., Brugamyer, E. J., Bryson, S. T., Carter, J. A., Ciardi, D. R., Howell, S. B., Steffen, J. H., Borucki, W. J., Koch, D. G., Winn, J. N., Welsh, W. F., Uddin, K., Tenenbaum, P., Still, M., Seager, S., Quinn, S. N., Mullally, F., Miller, N., Marcy, G. W., MacQueen, P. J., Lucas, P., Lissauer, J. J., Latham, D. W., Knutson, H., Kinemuchi, K., Johnson, J. A., Jenkins, J. M., Isaacson, H., Howard, A., Horch, E., Holman, M. J., Henze, C. E., Haas, M. R., Gilliland, R. L., Gautier, III, T. N., Ford, E. B., Fischer, D. A., Everett, M., Endl, M., Demory, B.-O., Deming, D., Charbonneau, D., Caldwell, D., Buchhave, L., Brown, T. M., & Batalha, N. 2011, ApJS, 197, 7

- Fabrycky, D. C., Ford, E. B., Steffen, J. H., Rowe, J. F., Carter, J. A., Moorhead, A. V., Batalha, N. M., Borucki, W. J., Bryson, S., Buchhave, L. A., Christiansen, J. L., Ciardi, D. R., Cochran, W. D., Endl, M., Fanelli, M. N., Fischer, D., Fressin, F., Geary, J., Haas, M. R., Hall, J. R., Holman, M. J., Jenkins, J. M., Koch, D. G., Latham, D. W., Li, J., Lissauer, J. J., Lucas, P., Marcy, G. W., Mazeh, T., McCauliff, S., Quinn, S., Ragozzine, D., Sasselov, D., & Shporer, A. 2012a, *ApJ*, 750, 114
- Fabrycky, D. C., Lissauer, J. J., Ragozzine, D., Rowe, J. F., Agol, E., Barclay, T., Batalha, N., Borucki, W., Ciardi, D. R., Ford, E. B., Geary, J. C., Holman, M. J., Jenkins, J. M., Li, J., Morehead, R. C., Shporer, A., Smith, J. C., Steffen, J. H., & Still, M. 2012b, *ArXiv e-prints*
- Ford, E. B., Fabrycky, D. C., Steffen, J. H., Carter, J. A., Fressin, F., Holman, M. J., Lissauer, J. J., Moorhead, A. V., Morehead, R. C., Ragozzine, D., Rowe, J. F., Welsh, W. F., Allen, C., Batalha, N. M., Borucki, W. J., Bryson, S. T., Buchhave, L. A., Burke, C. J., Caldwell, D. A., Charbonneau, D., Clarke, B. D., Cochran, W. D., Désert, J.-M., Endl, M., Everett, M. E., Fischer, D. A., Gautier, III, T. N., Gilliland, R. L., Jenkins, J. M., Haas, M. R., Horch, E., Howell, S. B., Ibrahim, K. A., Isaacson, H., Koch, D. G., Latham, D. W., Li, J., Lucas, P., MacQueen, P. J., Marcy, G. W., McCauliff, S., Mullally, F. R., Quinn, S. N., Quintana, E., Shporer, A., Still, M., Tenenbaum, P., Thompson, S. E., Torres, G., Twicken, J. D., Wohler, B., & the Kepler Science Team. 2012, *ApJ*, 750, 113
- Holman, M. J., Fabrycky, D. C., Ragozzine, D., Ford, E. B., Steffen, J. H., Welsh, W. F., Lissauer, J. J., Latham, D. W., Marcy, G. W., Walkowicz, L. M., Batalha, N. M., Jenkins, J. M., Rowe, J. F., Cochran, W. D., Fressin, F., Torres, G., Buchhave, L. A., Sasselov, D. D., Borucki, W. J., Koch, D. G., Basri, G., Brown, T. M., Caldwell, D. A., Charbonneau, D., Dunham, E. W., Gautier, T. N., Geary, J. C., Gilliland, R. L., Haas, M. R., Howell, S. B., Ciardi, D. R., Endl, M., Fischer, D., Fürész, G., Hartman, J. D., Isaacson, H., Johnson, J. A., MacQueen, P. J., Moorhead, A. V., Morehead, R. C., & Orosz, J. A. 2010, *Science*, 330, 51
- Holman, M. J. & Murray, N. W. 2005, *Science*, 307, 1288
- Lissauer, J. J., Ragozzine, D., Fabrycky, D. C., Steffen, J. H., Ford, E. B., Jenkins, J. M., Shporer, A., Holman, M. J., Rowe, J. F., Quintana, E. V., Batalha, N. M., Borucki, W. J., Bryson, S. T., Caldwell, D. A., Carter, J. A., Ciardi, D., Dunham, E. W., Fortney, J. J., Gautier, III, T. N., Howell, S. B., Koch, D. G., Latham, D. W., Marcy, G. W., Morehead, R. C., & Sasselov, D. 2011, *ApJS*, 197, 8
- Lithwick, Y. & Wu, Y. 2008, *arXiv 0802.2939*
- . 2012, “Resonant Repulsion of Kepler Planet Pairs,” *ArXiv*
- Murray, C. D. & Dermott, S. F. 2000, *Solar System Dynamics* (Cambridge University Press)
- Nesvorný, D. 2009, *ApJ*, 701, 1116
- Nesvorný, D. & Morbidelli, A. 2008, *ApJ*, 688, 636
- Ogilvie, G. I. 2007, *MNRAS*, 374, 131
- Papaloizou, J. C. B. 2011, *Celestial Mechanics and Dynamical Astronomy*, 111, 83
- Press, W. H., Teukolsky, S. A., Vetterling, W. T., & Flannery, B. P. 1992, *Numerical recipes in FORTRAN. The art of scientific computing* (Cambridge: University Press, —c1992, 2nd ed.)
- Steffen, J. H., Fabrycky, D. C., Ford, E. B., Carter, J. A., Désert, J.-M., Fressin, F., Holman, M. J., Lissauer, J. J., Moorhead, A. V., Rowe, J. F., Ragozzine, D., Welsh, W. F., Batalha, N. M., Borucki, W. J., Buchhave, L. A., Bryson, S., Caldwell, D. A., Charbonneau, D., Ciardi, D. R., Cochran, W. D., Endl, M., Everett, M. E., Gautier, T. N., Gilliland, R. L., Girouard, F. R., Jenkins, J. M., Horch, E., Howell, S. B., Isaacson, H., Klaus, T. C., Koch, D. G., Latham, D. W., Li, J., Lucas, P., MacQueen, P. J., Marcy, G. W., McCauliff, S., Middour, C. K., Morris, R. L., Mullally, F. R., Quinn, S. N., Quintana, E. V., Shporer, A., Still, M., Tenenbaum, P., Thompson, S. E., Twicken, J. D., & Van Cleve, J. 2012, *MNRAS*, 421, 2342
- Veras, D., Ford, E. B., & Payne, M. J. 2011, *ApJ*, 727, 74

APPENDIX  
DERIVATION OF ANALYTICAL TTV

We derive the transit time variations for two planets near a first order ( $j:j-1$ ) mean motion resonance, assuming that the planets are coplanar with each other and with the line of sight. We solve perturbatively, taking the following quantities to be small: the eccentricities ( $e, e'$ ), the mass ratios of the planets to the star ( $\mu, \mu'$ ) and the fractional distance to resonance ( $\Delta$ ). Typical values for Kepler planets are, very roughly  $e \lesssim 0.1$ ,  $\mu \lesssim 10^{-4}$ , and  $|\Delta| \lesssim 0.05$ . Section B provides further restrictions on these parameters for our perturbative treatment to be valid.

We first give a brief overview of the calculation that follows. When the equations of motion are solved perturbatively (where the unperturbed solution is circular), the leading order solution for the complex eccentricity is a sum of forced and free terms (Eq. A15); the leading order solution for the semimajor axis is determined by the product of the free and forced eccentricities (Eq. A19); and the perturbed solution for the longitudes is determined by the perturbed semimajor axis (divided by  $\Delta$ ; Eq. A22). These solutions determine the angular positions of the planets as functions of time (via Eq. A23). Finally, the angular positions are trivially inverted to obtain the times of transit, and hence the TTV.

The total energy, or Hamiltonian, is (e.g., Murray & Dermott 2000)

$$H = -\frac{GM_*m}{2a} - \frac{GM_*m'}{2a'} - \frac{Gmm'}{a'} R^j, \quad (\text{A1})$$

where  $M_*$  is the stellar mass, and the disturbing function due to the  $j:j-1$  resonance is

$$R^j = fe \cos(\lambda^j - \varpi) + ge' \cos(\lambda^j - \varpi'), \quad (\text{A2})$$

for

$$\lambda^j \equiv j\lambda' - (j-1)\lambda. \quad (\text{A3})$$

In the above,  $\{m, a, e, \lambda, \varpi, m', a', e', \lambda', \varpi'\}$  are the mass and standard orbital elements for the inner (unprimed) and outer (primed) planets, following the notation of Murray & Dermott (2000). The coefficients  $f$  and  $g$  are order-unity, and are functions of  $j$  and

$$\alpha \equiv a/a'. \quad (\text{A4})$$

These are tabulated for a few resonances in Table 3

The equations of motion are Hamilton's equations, after expressing the orbital elements in the above Hamiltonian in terms of canonical Poincaré variables (e.g. Murray & Dermott 2000). The resulting equation for the inner planet's longitude is

$$\frac{d\lambda}{dt} = \frac{1}{\sqrt{GM_*}} \frac{2\sqrt{a}}{m} \frac{\partial H}{\partial a} \quad (\text{A5})$$

$$\approx \sqrt{\frac{GM_*}{a^3}}, \quad (\text{A6})$$

and similarly for  $\lambda'$ . We drop the derivative of the disturbing function in the above, and justify this below. Variations in the semimajor axes are second order in eccentricity (see below); hence

$$\begin{pmatrix} \lambda \\ \lambda' \end{pmatrix} = \begin{pmatrix} \frac{2\pi}{P}(t-T) \\ \frac{2\pi}{P'}(t-T') \end{pmatrix} + \begin{pmatrix} \delta\lambda \\ \delta\lambda' \end{pmatrix} \quad (\text{A7})$$

where the periods are

$$P \equiv 2\pi\sqrt{\frac{a^3}{GM_*}}, \quad P' \equiv 2\pi\sqrt{\frac{a'^3}{GM_*}}. \quad (\text{A8})$$

The periods will henceforth be treated as constants (i.e., considered to be functions of the unperturbed semimajor axes);  $T$  and  $T'$  are constant reference times; and the variations in the longitudes  $\delta\lambda, \delta\lambda' = O(e^2)$  remain to be determined.

For the eccentricity equations, we introduce the complex eccentricities (e.g., Ogilvie 2007)

$$z \equiv ee^{i\varpi} \quad (\text{A9})$$

$$z' \equiv e'e^{i\varpi'}, \quad (\text{A10})$$

in terms of which the disturbing function may be written as

$$R^j = \frac{1}{2}(fz^* + gz'^*)e^{i\lambda^j} + \text{c.c.}, \quad (\text{A11})$$

where c.c. denotes the complex conjugate of the preceding term. The eccentricity equation for the inner planet is

$$\frac{dz}{dt} = -\frac{1}{\sqrt{GM_*}} \frac{2i}{m\sqrt{a}} \frac{\partial H}{\partial z^*} \quad (\text{A12})$$

to leading order in eccentricity, and similarly for the outer planet, i.e.

$$\frac{d}{dt} \begin{pmatrix} z \\ z' \end{pmatrix} = i \frac{2\pi}{P'} \begin{pmatrix} \mu' f / \sqrt{\alpha} \\ \mu g \end{pmatrix} e^{i\lambda^j} \quad (\text{A13})$$

where the mass ratios are

$$\mu \equiv m/M_*, \quad \mu' \equiv m'/M_*. \quad (\text{A14})$$

Solving the eccentricity equations to first order yields a sum of free and forced terms:

$$\begin{pmatrix} z \\ z' \end{pmatrix} = \begin{pmatrix} z_{\text{free}} \\ z'_{\text{free}} \end{pmatrix} - \frac{1}{j\Delta} \begin{pmatrix} \mu' f / \sqrt{\alpha} \\ \mu g \end{pmatrix} e^{i\lambda^j}, \quad (\text{A15})$$

where the free terms are constant and the normalized distance to resonance is

$$\Delta \equiv \frac{j-1}{j} \frac{P'}{P} - 1, \quad (\text{A16})$$

assumed to satisfy  $|\Delta| \ll 1$ . In the above, we have used the relation

$$\frac{d}{dt} \lambda^j = -(j\Delta) \frac{2\pi}{P'} + O(e^2) \quad (\text{A17})$$

We proceed to determine the  $O(e^2)$  changes to  $a, a'$ , and thereby to obtain  $\delta\lambda, \delta\lambda'$  to this order. To do so, we note that the resonant Hamiltonian (Equation (A1)) has two constants of motion in addition to the energy:  $K = \Lambda + (j-1)(\Gamma + \Gamma')$  and  $K' = \Lambda' - j(\Gamma + \Gamma')$ , where the  $\Lambda$  and  $\Gamma$  are the usual Poincaré momenta (Murray & Dermott 2000). From the constancy of  $K$ , the variation in  $a$  over the course of the planets' orbits (i.e.  $\delta a$ ) satisfies

$$m\sqrt{a} \frac{\delta a}{2a} + (j-1) \left( m\sqrt{a} \frac{e^2}{2} + m'\sqrt{a'} \frac{e'^2}{2} \right) = \text{const}, \quad (\text{A18})$$

discarding terms of higher order in  $\delta a, \delta a', e^2, e'^2$ . Inserting the eccentricities from Equation (A15), only the cross terms between the free and forced eccentricities yield time-varying components to  $\delta a$ , implying

$$\begin{pmatrix} \delta a/a \\ \delta a'/a' \end{pmatrix} = \begin{pmatrix} \frac{j-1}{j} \mu' / \sqrt{\alpha} \\ -\mu \end{pmatrix} \frac{Z_{\text{free}}^*}{\Delta} e^{i\lambda^j} + c.c. \quad (\text{A19})$$

where

$$Z_{\text{free}} \equiv f z_{\text{free}} + g z'_{\text{free}} \quad (\text{A20})$$

is a weighted sum of the two planets' free eccentricities.

The equation for the longitudes (Equation (A6)) becomes, to first order in  $\delta a$ ,

$$\frac{d}{dt} \delta\lambda = -\frac{3}{2} \frac{2\pi}{P} \frac{\delta a}{a}, \quad (\text{A21})$$

and similarly for the outer planet. The solutions are

$$\begin{pmatrix} \delta\lambda \\ \delta\lambda' \end{pmatrix} = \begin{pmatrix} \mu' \frac{j-1}{j} \alpha^{-2} \\ -\mu \end{pmatrix} \frac{3Z_{\text{free}}^*}{2ij\Delta^2} e^{i\lambda^j} + c.c., \quad (\text{A22})$$

Now, to convert from  $\lambda$  to  $\theta$ , we must add the following, valid to first order in eccentricity,

$$\theta - \lambda = 2e \sin(\lambda - \varpi) \quad (\text{A23})$$

$$= \frac{z^*}{i} e^{i\lambda} + c.c. \quad (\text{A24})$$

and similarly for primed quantities. Since we are ultimately interested in transit times, we need only insert for  $z$  the forced eccentricity (Equation (A15)), because the free eccentricity produces a term with the same period as the transits, and hence does produce variations from transit to transit. By the same logic, we may drop the  $e^{i\lambda}$  multiplying the forced eccentricity if we choose the observer to be at angular position 0. We then have

$$\begin{pmatrix} \theta - \lambda \\ \theta' - \lambda' \end{pmatrix} = \frac{1}{j\Delta} \begin{pmatrix} \mu' f / \sqrt{\alpha} \\ \mu g \end{pmatrix} \frac{e^{i\lambda^j}}{i} + c.c. \quad (\text{A25})$$

TABLE 3  
COEFFICIENTS OF THE DISTURBING FUNCTION, DEFINED VIA EQUATIONS (A1)–(A2). NUMERICAL VALUES EXPANDED TO FIRST ORDER IN  $\Delta$ , THE RELATIVE DISTANCE TO RESONANCE (EQ. A16).

	$j : j - 1^a$	2 : 1	3 : 2	4 : 3	5 : 4
$f$	$-jb_{1/2}^j - \frac{\alpha}{2}Db_{1/2}^j$	$-1.190 + 2.20\Delta$	$-2.025 + 6.21\Delta$	$-2.840 + 12.20\Delta$	$-3.650 + 20.15\Delta$
$g$	$(j - \frac{1}{2})b_{1/2}^{j-1} + \frac{\alpha}{2}Db_{1/2}^{j-1} + \text{indirect}_{2:1}$	$0.4284 - 3.69\Delta^b$	$2.484 - 5.99\Delta$	$3.283 - 11.9\Delta$	$4.084 - 19.86\Delta$

<sup>a</sup>  $b_s^j \equiv b_s^j(\alpha)$  are Laplace coefficients and  $D \equiv d/d\alpha$  (Murray & Dermott 2000).

<sup>b</sup> The 2:1 value of  $g$  contains the indirect term for an internal perturber ( $= -1/(2\alpha^2)$ ). One should use this in Equations (9)–(10) for the 2:1; however, in Equation (8) one should use  $Z_{\text{free}} = fz_{\text{free}} + g_{\text{ext}}z'_{\text{free}}$ , where  $g_{\text{ext}} = 0.4284 - 1.17\Delta$ , appropriate for an external perturber. Nonetheless, this distinction is unlikely to be of practical importance unless one is interested in the  $O(\Delta)$  corrections to the free eccentricities.

The final expression for  $\theta, \theta'$  is given by the sum of Equation (A7) (after inserting Equation (A22)) with Equation (A25), yielding

$$\theta = \frac{2\pi}{P}(t - T) - \frac{2\pi}{P} \left\{ \frac{V}{2i} e^{i\lambda^j} + c.c. \right\} \quad (\text{A26})$$

$$\theta' = \frac{2\pi}{P'}(t - T') - \frac{2\pi}{P'} \left\{ \frac{V'}{2i} e^{i\lambda^j} + c.c. \right\} \quad (\text{A27})$$

where the amplitudes are

$$V = \frac{P}{\pi} \frac{\mu'}{j\Delta} \alpha^{-1/2} \left( -f - \frac{j-1}{j} \alpha^{-3/2} \frac{3Z_{\text{free}}^*}{2\Delta} \right) \quad (\text{A28})$$

$$V' = \frac{P'}{\pi} \frac{\mu}{j\Delta} \left( -g + \frac{3Z_{\text{free}}^*}{2\Delta} \right). \quad (\text{A29})$$

Note that  $\alpha = \left( (1 + \Delta) \frac{j}{j-1} \right)^{-2/3}$ , whence follows Equation (8) in the body of the paper after dropping  $O(\Delta)$  corrections. (We somewhat inconsistently keep the  $O(\Delta)$  corrections to  $f$  and  $g$  in Table 3 because these can be quite large, especially near the 4:3 and 5:4 resonances). Since we choose  $\theta = 0$  to point along the line of sight, transits of the inner planet occur whenever  $\theta/2\pi = 0, 1, \dots$ , and similarly for the outer planet. We conclude that the TTV signals for the inner and outer planets are as given in Equations (1)–(10).

#### ASSUMPTIONS AND RANGE OF VALIDITY

- We have assumed the system is not locked in resonance. Resonance locking occurs when  $\delta\lambda \sim$  unity. From Equation (A22), this implies that our expressions are valid as long as

$$e_{\text{free}} \lesssim \Delta^2/\mu.$$

For typical Kepler systems,  $|\Delta| \gtrsim 1\%$  and  $\mu \lesssim 10^{-4}$ , and hence this assumption is usually valid.

- In Equation (A6), we dropped the derivative of the disturbing function. This term is  $\sim \mu e$ , and hence is smaller than the term that is kept by  $\sim \Delta$  (Eq. A21).
- We have neglected secular effects. Secular precession occurs on the timescale  $\sim P/\mu$ , which is much longer than the timescale of the resonant effects considered here,  $\sim P/\Delta$ . Hence secular effects only lead to corrections to our formulae of order  $|\mu/\Delta| \ll 1$ . Nonetheless, secular precession causes  $Z_{\text{free}}$  to precess on thousand-year timescales, which randomizes the orientation of  $Z_{\text{free}}$ . For that reason, we argue in this paper that if the data requires  $\angle Z_{\text{free}} = 0$  (or  $\pi$ ) for many systems, it suggests that their  $Z_{\text{free}}$  nearly vanishes.
- The timescale for general relativistic precession is also too long to be important, specifically  $(d\omega/dt)^{-1} \approx Pac^2/(6\pi GM_*) \approx 4000 \times P_{\text{day}}^{5/3}$  year/radian.
- We assume perfect coplanarity. The small inclination dispersion inferred for Kepler multi-planet systems justifies this assumption.